Published in final edited form as:
J Magn Reson Imaging. 2008 August ; 28(2): 445–452. doi:10.1002/jmri.21322.

Transit Delay and Flow Quantification in Muscle With Continuous Arterial Spin Labeling Perfusion-MRI

Wen-Chau Wu, PhD[1], **Jiongjiong Wang, PhD**[1], **John A. Detre, MD**[1,2], **Sarah J. Ratcliffe, PhD**[3], and **Thomas F. Floyd, MD**[2,4,*]

[1]Department of Radiology, Hospital of University of Pennsylvania, Philadelphia, Pennsylvania, USA.

[2]Department of Neurology, Hospital of University of Pennsylvania, Philadelphia, Pennsylvania, USA.

[3]Department of Biostatistics and Epidemiology, Hospital of University of Pennsylvania, Philadelphia, Pennsylvania, USA.

[4]Department of Anesthesiology and Critical Care, Hospital of University of Pennsylvania, Philadelphia, Pennsylvania, USA.

Abstract

Purpose—To test the hypothesis that flow measurements using continuous arterial spin labeling (CASL) magnetic resonance imaging (MRI) in muscle depend upon transit delay, and examine the repeatability of CASL measurements.

Materials and Methods—A total of 23 healthy subjects underwent CASL imaging of the calf, foot, and forearm with varying postlabeling delay (PLD = 1000, 1500, and 1900 msec). Experiments were conducted on a 3.0T system. An orthopedic tourniquet system was employed to create a five-minute period of ischemia followed by a transient hyperemic flow. Imaging commenced two minutes prior to cuff inflation and ended three minutes after cuff release.

Results—CASL was found able to well resolve the time course of the hyperemic flow pattern with an effective TR of 16 seconds, although we were unable to establish that a plateau had been reached in the flow measurements even at a PLD as long as 1900 msec. Peak hyperemic flow measurements compared favorably with those obtained with contrast-enhanced (CE) MRI following a similar period of ischemia. Region-of-interest (ROI)–based repeated measurements varied by approximately 20% over a period of one hour.

Conclusion—In all anatomic regions studied, flow measurements were found to increase with PLD, suggesting the prolonged transit delay in muscle.

Keywords

continuous arterial spin labeling; CASL; magnetic resonance; skeletal muscle; blood flow; hyperemia; transit delay

Flow within the microvasculature of muscle is altered in many disease states such as the vasculopathies of diabetes mellitus and peripheral vascular disease (1), the muscular dystrophies (2), myositis (3), and neoplasms (4). Microvascular flow (or perfusion) is hence

*Address reprint requests to: T.F.F., MD, Department of Anesthesiology & Critical Care, The Hospital of University of Pennsylvania, 3400 Spruce Street, Philadelphia, PA, USA. Thomas.Floyd@uphs.upenn.edu.

believed to be a measure more tightly coupled with physiology and pathophysiology as compared with blood oxygenation dependent (BOLD) contrast, a composite output of blood flow, blood volume, and oxygen consumption rate. Several techniques such as venous occlusion plethysmography (5), radionuclide plethysmography (6), thallium scintigraphy (7), positron emission tomography (PET) (8), and magnetic resonance imaging (MRI) (9–13) have been applied to measure skeletal muscle perfusion, yet there remains no gold standard. While plethysmography is probably the most widely used method, it only provides a global measurement and the technique may underestimate the true flow (14,15). Development of a reliable technique for perfusion measurement may assist in clinical decisions in dealing with critical limb ischemia (e.g., revascularization vs. amputation) and in assessing overall vascular health.

With MRI, muscle perfusion imaging can be achieved by first-pass contrast-enhanced (CE) imaging (9–11). The intravenous bolus injection of gadolinium chelates gives high signal-to-noise ratio (SNR) in CE-MRI but absolute flow quantification may be hindered by the uncertainty of the arterial input function. Alternatively, arterial spin labeling (ASL), originally developed for brain imaging (16), has been applied to measure skeletal muscle perfusion (12,13). Utilizing magnetically-labeled water as a tracer, this noninvasive method may benefit physiologic and pathophysiologic studies by virtue of the ability to repeat the study over tight time frames without tracer contamination. Somewhat unique to muscle is the low baseline flow (<10 mL/100 g/minute) (17), and rarely is this baseline flow particularly disturbed even in disease states. In light of this, and analogous to cardiac muscle, disease or functional capacity of this organ may be best tested under stress, which necessitates the use of paradigms such as exercise or temporary ischemia to allow measurement of flow or flow reserve in hyperdynamic or hyperemic states. While exercise presents unique MRI specific challenges, to include the need for gating of image acquisition, exercise may preferentially stimulate certain muscle groups more than others. This nonuniform stimulation across muscle groups and between subjects may not be optimal for pathophysiologic studies. An ischemic paradigm, created through the application of a brief tourniquet, may therefore be a better alternative for studies of the flow variability in diseased muscle. Quantification of hyperemic flow following a short period of ischemia has been found to be a valuable indicator of local (18,19) and systemic (20) vascular disease.

Frank et al (12) offered a detailed discussion of several potential difficulties in the application of ASL to the measurement of muscle flow, such as accurately accounting for the dynamic changes in relaxation times and water uptake during stress paradigms. They also acknowledged that studies have not rigorously examined the importance of the postlabeling delay (PLD) in the application of ASL to the muscle. In exercise and from ischemic paradigms, blood flow velocity may range form very low to very high levels, potentially resulting in a wide range of transit time as well as a dynamic range in labeling efficiency. These issues could be even more complicated in patients with peripheral vascular disease. In addition, the use of exercise paradigms (12,13) has made the investigation of ASL repeatability in skeletal muscle less straightforward. In view of this, an ischemic paradigm is adopted in the present study. We first test the hypothesis that continuous ASL (CASL) measurements in muscle depend upon transit delay. Secondly, we examine the repeatability of CASL measurements in muscle. Last, numerical simulations are conducted to estimate the impact of altered water uptake by muscle tissue upon flow quantification.

MATERIALS AND METHODS

Subjects and MR Experiments

With institutional review board (IRB) approval and appropriate consent obtained, 23 healthy subjects (35 ± 10 years of age, 11 women and 12 men) were recruited for this study, with no

history of smoking or diabetes mellitus, or evidence of vascular disease as assessed by the San Diego Walking Impairment Questionnaire (SWIQ) (21). All subjects were informed to avoid rigorous exercise in two hours before the study. Prior to entry, subjects underwent lower extremity systolic pressure measurements at multiple levels to include the calf, ankle, metatarsal, and toe. Pressures at these levels were indexed (or normalized) to the brachial artery as is typical when using these indices to identify the presence of vascular disease (22). Subjects then walked into the MR scanner room and were supine for approximately 15 minutes prior to scanning. To examine the importance of the PLD in flow quantification in muscle using CASL, subjects underwent imaging studies of the calf, foot, and forearm at varying PLDs. Due to the discomfort of the tourniquet and the time required to image each anatomical site, individuals were only able to contribute three to four sets of images during each one-hour session. Only rarely were we able to obtain a complete set of images (including three different PLDs) at all three anatomical sites of interest in a single individual ($N = 5$).

Studies were conducted on a 3.0T Siemens Trio whole-body MR system (Erlangen, Germany) with a custom designed dual-tuned proton/phosphorous transmit-receive knee coil (Nova Medical, Inc., Wakefield, MA, USA). A single-slice version of CASL sequence optimized for the field of 3T was used (23). The labeling plane was 6 cm proximal to the target slice in the tag experiment and 6 cm distal to the target slice in the control experiment to offset for magnetization transfer effect from the proximal tagging. Imaging parameters included: TR = 4 seconds, TE = 17 msec, tagging duration (τ) = 2 seconds, PLD = {1000, 1500, 1900} msec, field of view (FOV) = 22 cm, slice thickness = 1 cm, in-plane matrix size = 64 × 64, single-shot gradient-echo echo-planar readout. A high-resolution magnetization prepared rapid gradient echo (MPRAGE) or two-dimensional (2D) spoiled gradient-echo (SPGRE) anatomic image was also obtained for flow quantification in muscle and vascular regions of interest (ROIs).

Subjects were placed supine, with the knee slightly flexed for studies of the mid-calf and trans-metatarsal images. Subjects were placed prone in the swimming position for mid-forearm imaging. Extremities were positioned within the coil and fixed in position within a VacFix® vacuum cushion bead bag (PAR Scientific A/S, Houston, TX, USA). A tourniquet system with nonmagnetic cuff placed on the thigh or upper arm was utilized at 250 mmHg to create a five-minute period of ischemia followed by a transient hyperemic flow. The ischemic period was chosen because the magnitude of the hyperemic response has not been found to further increase beyond a five-minute ischemic period (15) even though muscle O_2 is exhausted after approximately six minutes of ischemia (24). Imaging commenced two minutes prior to tourniquet inflation and ended three minutes after tourniquet release.

Data Processing

Postprocessing was performed using VOXBO (http://www.voxbo.org) and software written in IDL (RSI, Boulder, CO, USA), which included a motion correction algorithm, and utilized the appropriate MPRAGE or 2D SPGRE anatomic image to hand-draw ROIs encompassing the soleus muscle of the calf and flexor muscle groups of the forearm and foot (plantar) flexors. Flow was calculated by Eq. [1]

$$f = \frac{\lambda \Delta M}{2\alpha T_1 M_0 \left[\exp\left(-\frac{PLD}{T_1}\right) - \exp\left(-\frac{PLD+T}{T_1}\right)\right]}, \quad [1]$$

in which ΔM was the signal difference between tag and control images, and M_0 was the blood signal at thermal equilibrium. The α (tagging efficiency) and λ (blood/tissue partition

coefficient) were assumed to be 0.9 (25) and 0.9 mL/g (26), respectively. Based on the single-compartment model, the T_1 of blood was chosen to be 1600 msec (27). In other words, the scenario was simplified by assuming that all tagged spins were restricted to the intravascular space without exchanging into tissue interstitium or intracellular space. The potential errors were later evaluated with numerical simulations. Because the paradigm of cuff occlusion could induce relatively large dynamic changes in raw images, the pair-wise subtraction between successive label and control acquisitions was prone to contamination from the changes in the "static" signals. To minimize this confound, the control image series were first linearly interpolated so that the pair-wise subtraction was carried out using temporally matched label and control images. To eliminate the residual static signal between label and control acquisitions caused by imperfect gradients, the polarity of gradients was flipped every pair of label and control acquisitions. After subtraction, two adjacent data points were averaged, resulting in an effective temporal resolution of 16 seconds. Peak and mean hyperemic flow (mL/100 g/minute), hyperemic blood volume (mL/100 g), time to peak (seconds), and hyperemic flow duration (seconds) were calculated for each anatomic ROI. The average flow over the central three minutes of the five-minute cuff inflation period referred to the zero level of flow. As illustrated in Fig. 1, hyperemic flow duration was measured from the initial positive deflection above the zero level following cuff deflation to the return to this same baseline. Mean hyperemic flow and hyperemic flow volume were defined as the average flow and flow integral, respectively. Mean time values were rounded to the nearest 16-second interval. It is worth mentioning that distal tagging could result in labeling the venous blood originating in muscle or large veins distal to the imaging plane. Distally labeled venous tags, if able to reach the control image, could theoretically lead to flow underestimation and even negative ASL signals. Since any signals arising from distal venous labeling would be confined to large collecting veins from distal draining venules, they could likely be easily distinguished and eliminated in ROI analysis.

Statistics and Reproducibility

To examine the reproducibility, eight subjects underwent aforementioned CASL measurements twice, one hour apart. Anatomical sites were marked to allow uniformity in repeated imaging. The within-subject coefficient of variation, $wsCV = \sqrt{[}$Mean of the $(wsSD/\text{subject mean flow})^2]$ was calculated following the guidelines proposed by Bland and Altman (28) for determining measurement error or precision.

Mean and standard deviations (SDs) were calculated for each of the tested variables. An analysis of variance (ANOVA) linear regression approach was used to test the dependence of the measured variables upon muscle group (i.e., ROI) and PLD. Flow ratios were calculated from population means at each ROI divided by population means in the forearm flexors at each PLD.

Computer Simulation: Effects of T_1/T_2 and Water Extraction

The success of flow quantification using ASL requires knowledge of several factors such as water exchange fraction from blood to interstitial space and the relaxation times (T_1, T_2, or T_2*) of blood and tissue. While T_1 for blood and muscle are close at 3T (1600 (27) vs. 1400 (29) msec), T_2 differs significantly between resting muscle (~50 msec) and oxygenated blood (275 msec) (29). Computer simulations were conducted to estimate the potential errors arising from these factors. Water extraction rates from 0% to 100% were considered to account for different relaxation times of blood and muscle (assuming T_1/T_2* = 1600 msec/100 msec for blood and 1400 msec/30 msec for muscle). For a given flow (f_0), ASL signal (i.e., signal difference between tag and control images) was generated by Eq. [1] and whereby flow was calculated (f_{cal}) under the condition described in data processing (i.e., no water extraction). Apparent flow, the ratio of f_{cal} to f_0, was computed for PLDs of 1000

msec, 1500 msec, and 1900 msec. For simplicity, no outflow (or venous shunting) was accounted for in the calculation (see Discussion for rationale). One would expect higher possibility of water exchange at longer PLD. But due to the lack of reference for data of exchange time (T_{ex}: the time after a tag enters the capillary bed before it exchanges to extravascular space) in muscle, the T_{ex} effect was ignored in the simulation. As a consequence, the calculated errors were the worst case.

RESULTS

Brachial, ankle, metatarsal, and toe systolic pressures were measured in 17 of 23 participants. The ankle vs. brachial (ABI), metatarsal vs. brachial (MBI), and toe vs. brachial (TBI) systolic pressure indices were 1.15 ± 0.10, 1.08 ± 0.26, and 0.92 ± 0.22, respectively. Values above 0.9 were considered to reflect minimal or nonexistent disease. SWIQ was also implemented to identify the presence of claudication. None of the 23 subjects gave a history consistent with claudication. Thus, two independent vascular disease diagnostic criteria confirmed the health of the subjects under study.

Mean CASL flow images during the postischemic hyperemia from a single subject are depicted in Fig. 2 (Fig. 2a, calf; b, forearm; and c, foot). Exceptional intensity is observed in the soleus muscle relative to surrounding muscle groups. Figure 3 shows the *group* mean hyperemic flow-time courses obtained with different PLDs (1000 msec, 1500 msec, and 1900 msec): Fig. 3a shows the soleus muscle in the calf; Fig. 3b, the flexors of the forearm; and Fig. 3c, the plantar flexors of the foot. One notices that the peak flow increases with increasing PLD in all locations. In Fig. 4, *group* mean and peak hyperemic flows are depicted as bar charts for the three ROIs at PLDs of 1000 msec, 1500 msec, and 1900 msec, again demonstrating the consistent pattern of increasing flow measurements with increasing PLD. To compare the flow patterns between anatomic locations, hyperemic flow-time series obtained with 1900-msec PLD from three different regions are overlaid in Fig. 5. Flow in the plantar flexors appears to peak later and the hyperemic duration is longer than in soleus or forearm flexors.

For each anatomic location and PLD, the aforementioned indices are calculated and summarized in Table 1. In the brackets are the ratio of soleus and plantar flexor to forearm flexor. A detailed statistical analysis has been performed in the form of a two-way ANOVA with interaction effect. The results of this statistical interpretation are found in Table 2. In this analysis, we test the hypothesis that peak flow, mean flow, total flow, time to peak, and peak width (hyperemic duration) are dependent upon both ROI and PLD, and we test the interaction between the variables. The analysis confirms that peak flow, mean flow, and total flow are dependent upon ROI as well as PLD. While time to peak is dependent upon ROI, it is not dependent upon PLD, and peak width is dependent upon neither. Finally, the wsCV from the soleus muscle of the calf was 24% for peak flow measurements.

Figure 6 shows the estimated error arising from the use of a single-compartment model based on blood pool alone. Underestimation occurs when tags exchange into tissue as a consequence of short T_1/T_2* in muscle. The effect is predicted to be larger at longer PLDs although the PLD-dependent difference is rather small.

DISCUSSION

We employed CASL to measure blood perfusion in human calf, foot, and forearm. In all anatomic regions studied, flow measurements were found to increase with PLD. We were not able to establish that a plateau had been reached in the flow measurements even at a PLD as long as 1900 msec. Nevertheless, CASL was able to reasonably well resolve the

time course of the hyperemic flow pattern even with an effective TR interval of 16 seconds. Repeated measurements within the soleus muscle ROI varied by approximately 20% over the period of one hour. The comparison of within-subject reproducibility of perfusion measurements, however, is not straightforward because of the different measure modalities, statistical analyses, and target organs in literature. Previous ASL studies demonstrated a variability of 5.8% in whole brain and 15% in territorial ROI (30). The lower degree of reproducibility in ROI-based analysis indicated the statistical effect of sampling a small population of pixels. Velocity-encoded phase-contrast MRI yielded tight inter- and intraobserver correlation in flow measurements while within-subject variation was also high (26%) (31). With venous occlusion plethysmography, a variation of 6% to 20% has been reported in repeated measurements of postischemic hyperemia in the whole calf (32,33). The variation may be up to 50% for flow-mediated dilation (34) in which the change in the diameter of brachial artery is measured in response to a similar ischemic challenge. More recently, perfusion was measured with ASL and diffuse light spectroscopy simultaneously in human calf (35). A variability of 8% was reported for both methods at a time frame of 10 minutes in addition to a nice correlation between two methods ($R^2 = 0.64$). These observations suggest that most of the variability between measurements is secondary to physiologic variability and that the hyperemic paradigm may induce a considerable range of physiologic variability that should be taken into account.

Peak hyperemic flow measurements obtained in our experiments compare favorably with those obtained with CE-MRI following a similar period of ischemia (9) that yielded values of 184.3 ± 41.3 mL/100 g/minute for the soleus muscle, and 122.4 ± 34.4 mL/100 g/minute for the tibialis anterior. Several other investigations of muscle flow using ASL exist. Toussaint et al (36) applied a five-minute period of ischemia prior to the measurement of the hyperemic blood flow response in the calf and reported peak flow values in soleus and gastrocnemius of 120 ± 63 and 116 ± 94 mL/100 g/minute, respectively. They also reported a time to peak of 22 ± 7 seconds and an ischemic period of 97 ± 47 seconds. Lebon et al (37) employed a seven-minute ischemic period to the calf and measured a peak perfusion (averaged across the entire calf) of 123 ± 42 mL/100 g/minute and a mean perfusion of 57 ± 16 mL/100 g/minute during the initial minute following reperfusion.

Exercise and postischemic hyperemia markedly increases flow rates (38). At very high flow rates, labeling efficiency could be compromised. Macotta et al (39) has demonstrated theoretically wide ranges in flow velocity (~20–150 cm/second) over which adiabatic inversion efficiency is ~90%. Unpublished data from our laboratory indicates that flow velocity within the popliteal artery increases from 50 cm/second at baseline to approximately 100 cm/second immediately following cuff deflation and returns to baseline within 45–60 seconds. This range of flows is well within the efficacious range for adiabatic labeling described by Macotta et al (39).

To accurately quantify flow with ASL, a sufficiently long PLD is necessary to allow for proximal tags to reach capillary bed. If the PLD is too short, ASL signal may be spatially biased toward the arterial watershed and tissue perfusion can be underestimated. However, it is notable that although measured flows (both peak and mean) increased with longer PLD (discussed in the next paragraph), *calf or foot* flow ratios, when referenced to forearm flexor flow, did not appreciably change with PLD (see the brackets in Table 1). For reasons that are unclear, atherosclerosis largely spares the upper extremity. Jondeau et al (40) has demonstrated that the hyperemic forearm flow response is preserved in subjects with heart failure even when the calf flow response diminishes. Because of this fact, the ratio of segmental systolic pressures in the lower extremity to the systolic pressure in the brachial artery appears to be a reliable index of vascular disease. The ratio of CASL-measured tissue flow in the lower extremity to that in the upper extremity may also have diagnostic value.

The success of flow quantification using ASL also requires knowledge of water exchange fraction. The measurement of water exchange fraction remains a challenge, especially with a wide range of flow velocities in addition to the fact that tags can leave capillary bed via draining to the venous system. To estimate the potential errors in our measurement using a single-compartment model (blood pool alone), we conducted computer simulations and found that flow could be underestimated in the presence of water extraction due to the shorter T_1/T_2* in muscle (Fig. 6). The effect is larger at longer PLDs but the PLD-dependent difference is predicted to be small. The muscular T_2* change accompanying ischemia (<5 msec, Ref. 37) is a minor issue, relative to the T_2* change caused by water extraction (e.g., 10% exchange corresponds to 10 msec variation in T_2*). Flow underestimation could also occur if tagged spins leave the target slices prior to image acquisition. The elevated flow velocities following cuff deflation may allow less time for water exchange between intra- and extravascular spaces, and may shorten the time that blood takes to traverse the capillary bed. In muscle at baseline, it has been documented that 40% of radioactively-labeled arterial blood bypasses the muscle bed and is shunted into the venous system (41). Considering the PLD used in our experiment (<2 seconds) and that capillary transit time in muscle is on the order of one to five seconds (9,42), the signal from the shunted tags would likely still be within the imaging plane at the time of image acquisition and would be indistinguishable from those tags that had entered muscle. In this scenario, the measured flow “value” remains unaffected but the spatial distribution of flow is biased toward the venous system. In the event that the longer PLD allows for a greater volume of spins to exchange into muscle where resting T_1 is less than in blood, one would expect greater attenuation of signal and therefore flow underestimation as predicted in Fig. 6. It therefore appears that the only explanation for the greater signal measured at the longer PLD is that the transit delay in muscle is indeed prolonged.

We showed in this study that CASL allowed visualization of flow patterns in all anatomic regions studied, especially at longer PLD, although it was not able to be determined at what PLD flow would plateau, probably due to prolonged transit time in muscle. What at first may seem a limitation in the technique, the flow variance with PLD may ultimately be used to diagnostic advantage, as it is likely that the slope of this variance will be impacted by the severity of disease. Furthermore, even though peak measured flows increased with longer PLD, the flow at each ROI, when referenced to flow in the forearm and expressed as a flow ratio, did not appreciably change. Thus, given the fact that flow in the forearm is preserved even in the presence of severe vascular disease, CASL, though potentially limited in its ability to accurately document absolute flow under certain circumstances, may allow accurate determination of the flow ratio.

In conclusion, the application of CASL to the study of the microvascular bed may allow unique and important insight into the pathogenesis and progression of disease in patients with peripheral vascular disease and diabetes mellitus. This preliminary study provides a foundation for further testing and application of the CASL approach as a noninvasive diagnostic and research tool in these disorders.

Acknowledgments

Contract grant sponsor:; Contract grant number: NIH-R01HL075649-01; Contract grant sponsor:; Contract grant number: NIH-RR002305.

REFERENCES

1. Rattigan S, Bussey CT, Ross RM, Richards SM. Obesity, insulin resistance, and capillary recruitment. Microcirculation. 2007; 14:299–309. [PubMed: 17613803]

2. Jensen TD, Kazemi-Esfarjani P, Skomorowska E, Vissing J. A forearm exercise screening test for mitochondrial myopathy. Neurology. 2002; 58:1533–1538. [PubMed: 12034793]
3. Weber MA, Krix M, Jappe U, et al. Pathologic skeletal muscle perfusion in patients with myositis: detection with quantitative contrast-enhanced US—initial results. Radiology. 2006; 238:640–649. [PubMed: 16371585]
4. Cuenod CA, Fournier L, Balvay D, Guinebretiere JM. Tumor angiogenesis: pathophysiology and implications for contrast-enhanced MRI and CT assessment. Abdom Imaging. 2006; 31:188–193. [PubMed: 16447089]
5. Rose SC. Noninvasive vascular laboratory for evaluation of peripheral arterial occlusive disease: Part I—hemodynamic principles and tools of the trade. J Vasc Interv Radiol. 2000; 11:1107–1114. [PubMed: 11041465]
6. Wolfram RM, Budinsky AC, Sinzinger H. Assessment of peripheral arterial vascular disease with radionuclide techniques. Semin Nucl Med. 2001; 31:129–142. [PubMed: 11330784]
7. Wada O, Asanoi H, Miyagi K, et al. Quantitative evaluation of blood flow distribution to exercising and resting skeletal muscles in patients with cardiac dysfunction using whole-body thallium-201 scintigraphy. Clin Cardiol. 1997; 20:785–790. [PubMed: 9294671]
8. Kalliokoski KK, Kemppainen J, Larmola K, et al. Muscle blood flow and flow heterogeneity during exercise studied with positron emission tomography in humans. Eur J Appl Physiol. 2000; 83:395–401. [PubMed: 11138581]
9. Thompson RB, Aviles RJ, Faranesh AZ, et al. Measurement of skeletal muscle perfusion during postischemic reactive hyperemia using contrast-enhanced MRI with a step-input function. Magn Reson Med. 2005; 54:289–298. [PubMed: 16032661]
10. Lutz AM, Weishaupt D, Amann-Vesti BR, et al. Assessment of skeletal muscle perfusion by contrast medium first-pass magnetic resonance imaging: technical feasibility and preliminary experience in healthy volunteers. J Magn Reson Imaging. 2004; 20:111–121. [PubMed: 15221816]
11. Nygren AT, Greitz D, Kaijser L. Skeletal muscle perfusion during exercise using Gd-DTPA bolus detection. J Cardiovasc Magn Reson. 2000; 2:263–270. [PubMed: 11545125]
12. Frank LR, Wong EC, Haseler LJ, Buxton RB. Dynamic imaging of perfusion in human skeletal muscle during exercise with arterial spin labeling. Magn Reson Med. 1999; 42:258–267. [PubMed: 10440950]
13. Boss A, Martirosian P, Claussen CD, Schick F. Quantitative ASL muscle perfusion imaging using a FAIR-TrueFISP technique at 3.0T. NMR Biomed. 2006; 19:125–132. [PubMed: 16404727]
14. Bystrom S, Jensen B, Jensen-Urstad M, Lindblad LE, Kilbom A. Ultrasound-Doppler technique for monitoring blood flow in the brachial artery compared with occlusion plethysmography of the forearm. Scand J Clin Lab Invest. 1998; 58:569–576. [PubMed: 9890340]
15. Hiatt WR, Huang SY, Regensteiner JG, et al. Venous occlusion plethysmography reduces arterial diameter and flow velocity. J Appl Physiol. 1989; 66:2239–2244. [PubMed: 2745287]
16. Detre JA, Leigh JS, Williams DS, Koretsky AP. Perfusion imaging. Magn Reson Med. 1992; 23:37–45. [PubMed: 1734182]
17. Elia M, Kurpad A. What is the blood flow to resting human muscle? Clin Sci (Lond). 1993; 84:559–563. [PubMed: 8504633]
18. Hummel BW, Hummel BA, Mowbry A, Maixner W, Barnes RW. Reactive hyperemia vs. treadmill exercise testing in arterial disease. Arch Surg. 1978; 113:95–98. [PubMed: 619865]
19. Dorigo B, Bartoli V, Grisillo D, Beconi D, Zanini A. Exercise hyperemia for the study of peripheral circulation. Angiology. 1980; 31:50–57. [PubMed: 7369539]
20. Poredos P, Golob M, Jensterle M. Interrelationship between peripheral arterial occlusive disease, carotid atherosclerosis and flow mediated dilation of the brachial artery. Int Angiol. 2003; 22:83–87. [PubMed: 12771862]
21. Regensteiner JG, Steiner JF, Panzer RJ, Hiatt WR. Evaluation of walking impairment by questionnaire in patients with peripheral arterial disease. J Vasc Med Biol. 1990; 2:142–152.
22. McDermott MM, Greenland P, Liu K, et al. The ankle brachial index is associated with leg function and physical activity: the walking and leg circulation study. Ann Intern Med. 2002; 136:873–883. [PubMed: 12069561]

23. Alsop DC, Detre JA. Reduced transit-time sensitivity in noninvasive magnetic resonance imaging of human cerebral blood flow. J Cereb Blood Flow Metab. 1996; 16:1236–1249. [PubMed: 8898697]
24. Wang ZY, Noyszewski EA, Leigh JS Jr. In vivo MRS measurement of deoxymyoglobin in human forearms. Magn Reson Med. 1990; 14:562–567. [PubMed: 2355838]
25. Williams DS, Detre JA, Leigh JS, Koretsky AP. Magnetic resonance imaging of perfusion using spin inversion of arterial water. Proc Natl Acad Sci USA. 1992; 89:212–216. [PubMed: 1729691]
26. Herscovitch P, Raichle ME. What is the correct value for the brain-blood partition coefficient for water. J Cereb Blood Flow Metab. 1985; 5:65–69. [PubMed: 3871783]
27. Greenman RL, Shirsoky JE, Mulkern RV, Rofsky NM. Double inversion black-blood fast spin-echo imaging of the human heart: a comparison between 1.5T and 3.0T. J Magn Reson Imaging. 2003; 17:648–655. [PubMed: 12766893]
28. Bland JM, Altman DG. Measurement error. BMJ. 1996; 313:744. [PubMed: 8819450]
29. Stanisz GJ, Odrobina EE, Pun J, et al. T1, T2 relaxation and magnetization transfer in tissue at 3T. Magn Reson Med. 2005; 54:507–512. [PubMed: 16086319]
30. Floyd TF, Ratcliffe SJ, Wang J, Resch B, Detre JA. Precision of the CASL-perfusion MRI technique for the measurement of cerebral blood flow in whole brain and vascular territories. J Magn Reson Imaging. 2003; 18:649–655. [PubMed: 14635149]
31. Klein WM, Bartels LW, Bax L, van der Graaf Y, Mali WP. Magnetic resonance imaging measurement of blood volume flow in peripheral arteries in healthy subjects. J Vasc Surg. 2003; 38:1060–1066. [PubMed: 14603218]
32. Thijssen DH, Bleeker MW, Smits P, Hopman MT. Reproducibility of blood flow and post-occlusive reactive hyperaemia as measured by venous occlusion plethysmography. Clin Sci (Lond). 2005; 108:151–157. [PubMed: 15494042]
33. Altenkirch HU, Fransson L, Koch G. Assessment of arterial and venous circulation in upper and lower extremities by venous occlusion strain gauge plethysmography. Normal values and reproducibility. Vasa. 1989; 18:140–145. [PubMed: 2741535]
34. De Roos NM, Bots ML, Schouten EG, Katan MB. Within-subject variability of flow-mediated vasodilation of the brachial artery in healthy men and women: implications for experimental studies. Ultrasound Med Biol. 2003; 29:401–406. [PubMed: 12706191]
35. Yu G, Floyd TF, Durduran T, et al. Validation of diffuse correlation spectroscopy for muscle blood flow with concurrent arterial spin labeling perfusion. Opt Express. 2007; 15:1064–1075. [PubMed: 19532334]
36. Toussaint JF, Kwong KK, Mkparu FO, et al. Perfusion changes in human skeletal muscle during reactive hyperemia measured by echo-planar imaging. Magn Reson Med. 1996; 35:62–69. [PubMed: 8771023]
37. Lebon V, Carlier PG, Brillault-Salvat C, Leroy-Willig A. Simultaneous measurement of perfusion and oxygenation changes using a multiple gradient-echo sequence: application to human muscle study. Magn Reson Imaging. 1998; 16:721–729. [PubMed: 9811138]
38. Rowell LB. Muscle blood flow in humans: how high can it go? Med Sci Sports Exerc. 1988; 20:S97–S103. [PubMed: 3057322]
39. Maccotta L, Detre JA, Alsop DC. The efficiency of adiabatic inversion for perfusion imaging by arterial spin labeling. NMR Biomed. 1997; 10:216–221. [PubMed: 9430351]
40. Jondeau G, Katz SD, Toussaint JF, et al. Regional specificity of peak hyperemic response in patients with congestive heart failure: correlation with peak aerobic capacity. J Am Coll Cardiol. 1993; 22:1399–1402. [PubMed: 8227797]
41. Johnson JA, Cavert HM, Lifson N. Kinetics concerned with distribution of isotopic water in isolated perfused dog heart and skeletal muscle. Am J Physiol. 1952; 171:687–693. [PubMed: 13016819]
42. Kalliokoski KK, Knuuti J, Nuutila P. Blood transit time heterogeneity is associated to oxygen extraction in exercising human skeletal muscle. Microvasc Res. 2004; 67:125–132. [PubMed: 15020203]

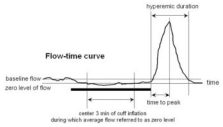

Figure 1.

Schematic illustration of the indexes measured in this study. The thick horizontal line indicates the five-minute cuff inflation. The average flow over the center three minutes is chosen to be the zero level while the average flow before cuff inflation is defined as the baseline. The hyperemic flow volume is the flow integral in hyperemic duration that is measured from the first positive deflection after cuff release to the time when flow returns to zero level.

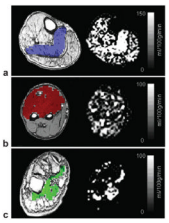

Figure 2.
Axial anatomic 2D SPGRE image with colored ROI and CASL mean hyperemic flow images from the three imaging sites: (**a**) calf-mid (soleus-ROI), (**b**) forearm-mid (forearm flexors-ROI), and (**c**) foot-transmetatarsal (plantar flexors-ROI).

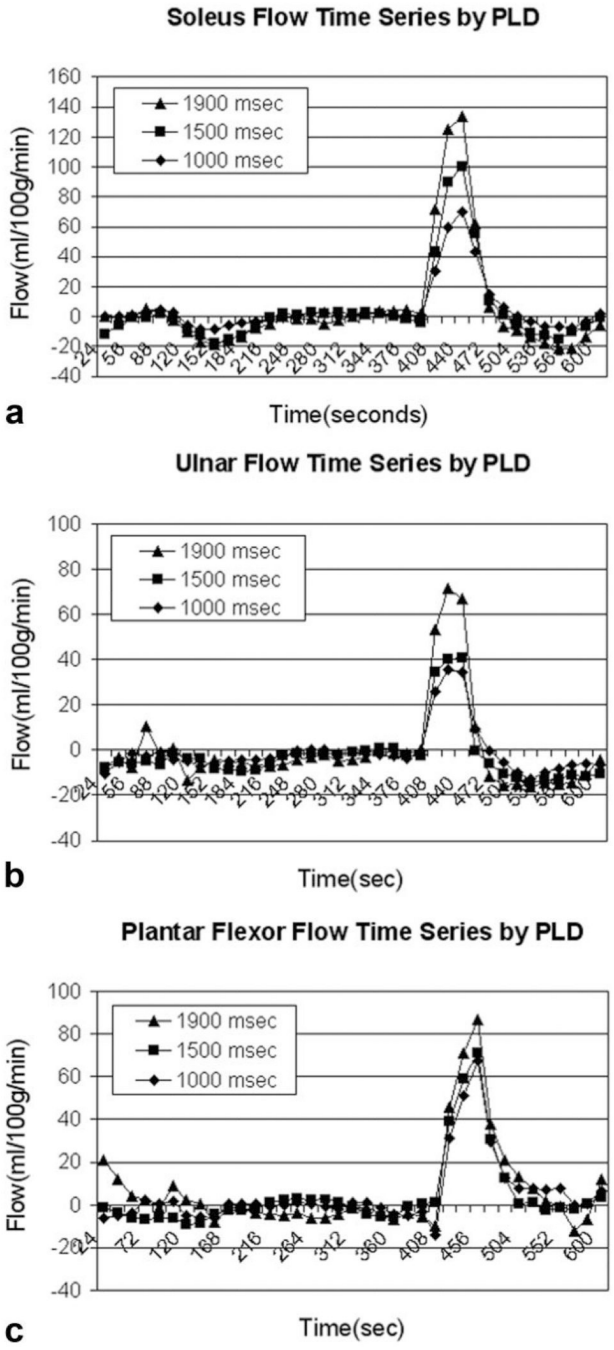

Figure 3.

Overlaid flow-time series with PLD = 1000, 1500, and 1900 msec for mid-calf, forearm, and plantar flexors (**a**–**c**, respectively). Absolute flow estimates were plotted against time in 16-second intervals for each anatomic location at the multiple PLDs.

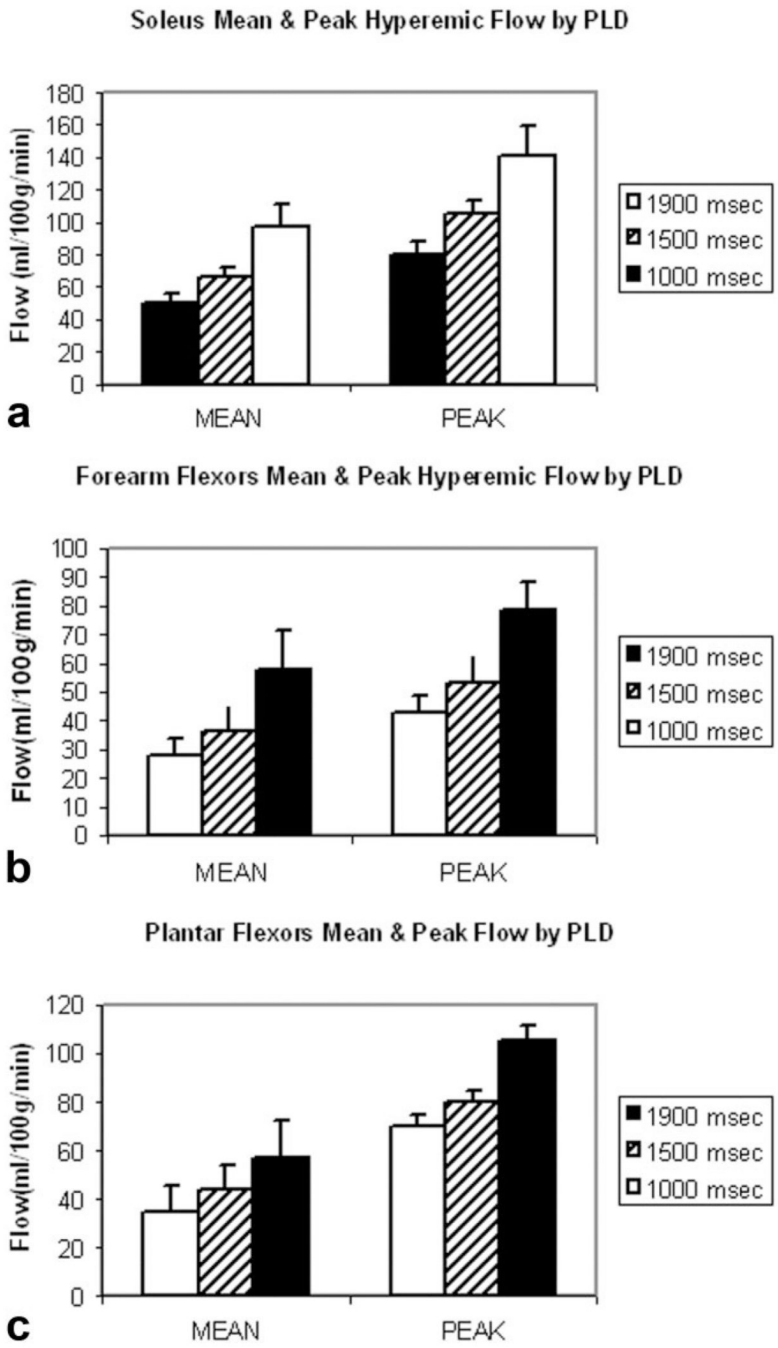

Figure 4.
Mean and peak hyperemic flow at varying PLDs by ROI: (**a**) soleus, (**b**) forearm flexors, and (**c**) plantar flexors.

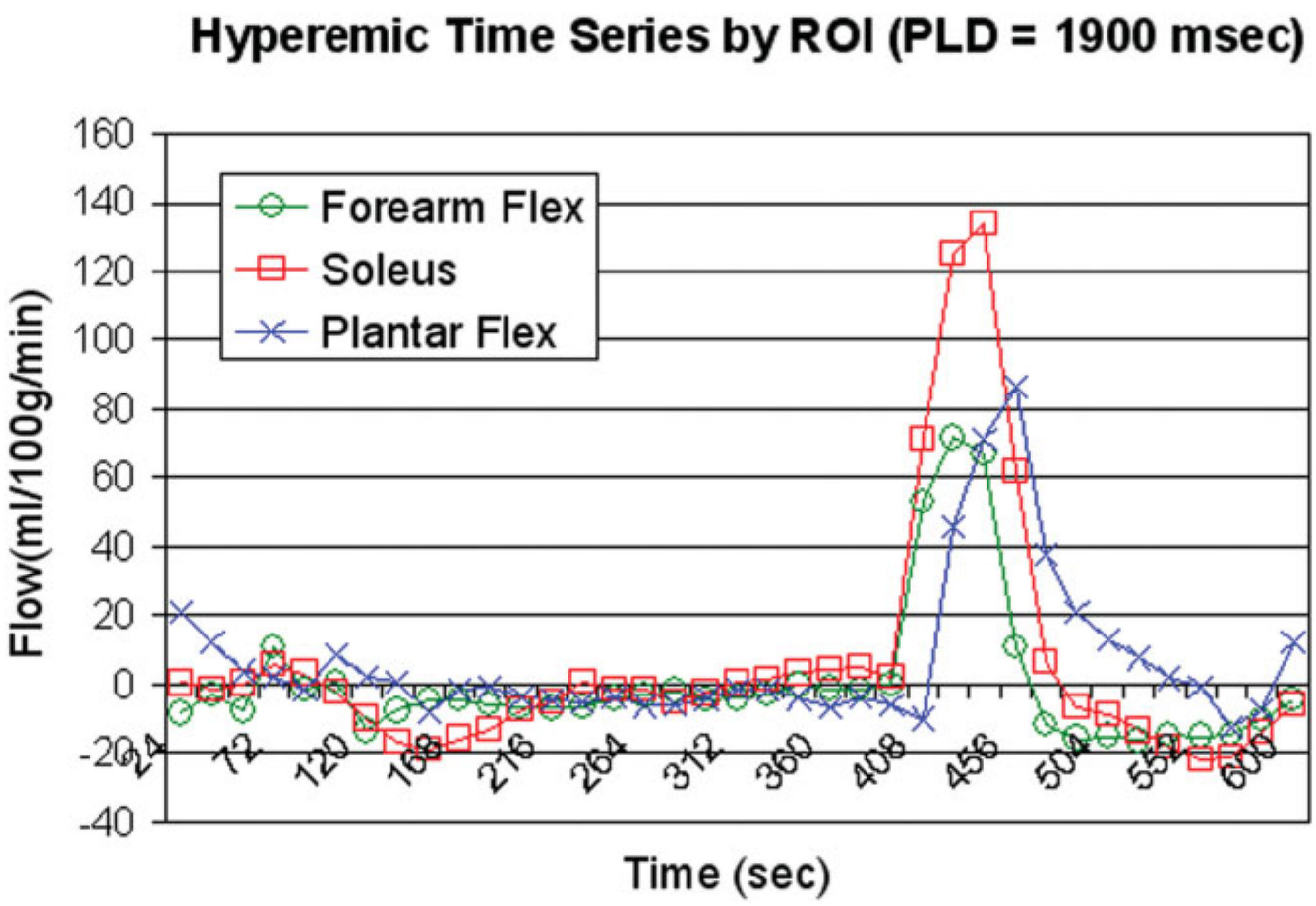

Figure 5.
Overlaid CASL time series from soleus, plantar flexors, and forearm flexors at 1900 msec.

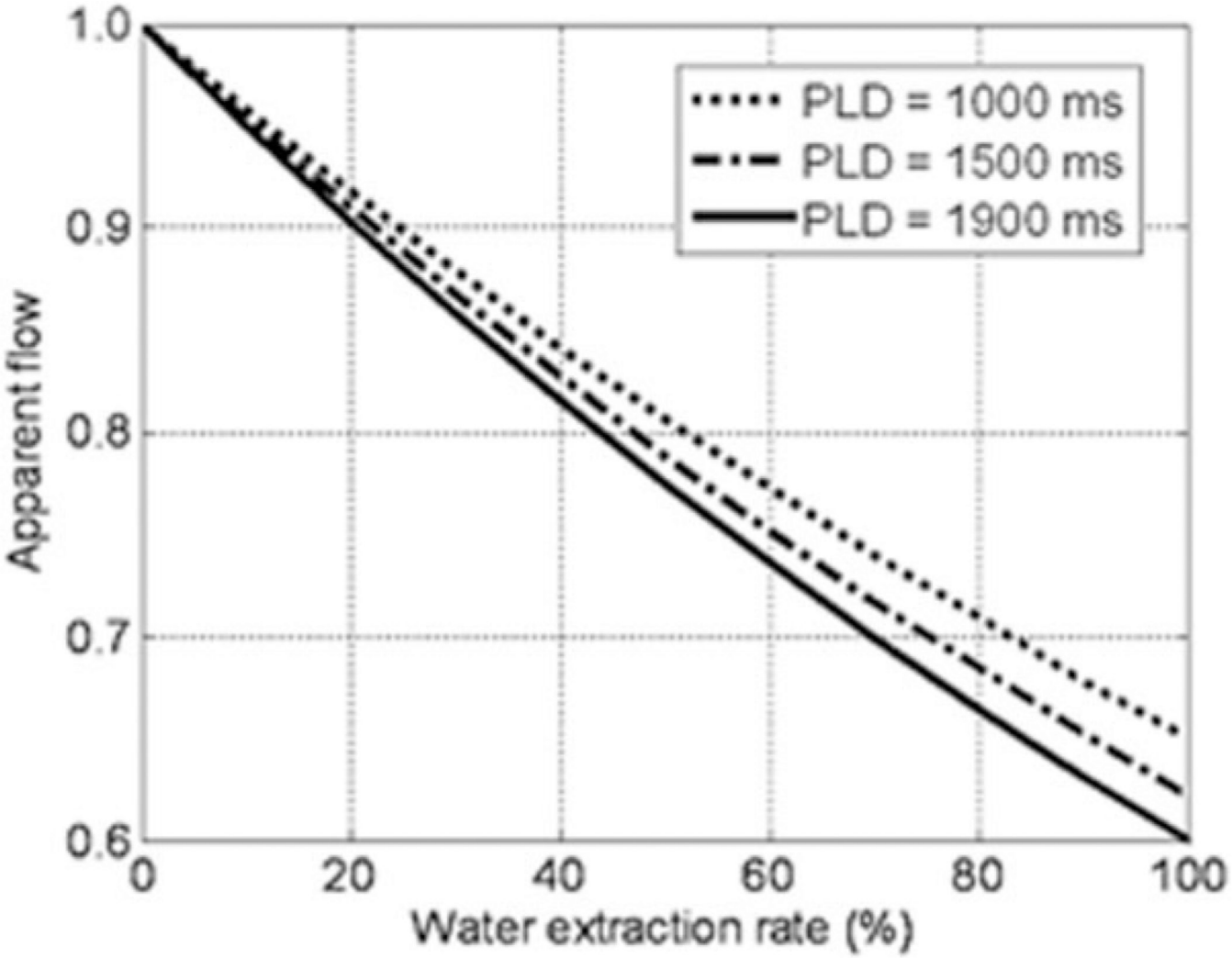

Figure 6.
Simulated quantitative errors caused by water extraction. The calculation of apparent flow is described in the computer simulations discussed in Materials and Methods.

Table 1

Summary of Flow Measurements*

Anatomy	PLD (msec)	*N*	Hyperemic indexes				
			Peak flow (mL/100 g/min)	**Mean flow (mL/100 g/min)**	**Flow volume (mL/100 g)**	**Time to peak (sec)**	**Peak width (sec)**
Mid-calf (soleus)	1000	12	80 ± 31 [1.9]	51 ± 19 [1.8]	63 ± 27 [2.3]	48 ± 14	75 ± 17
	1500	10	104 ± 25 [2.0]	66 ± 18 [1.8]	85 ± 20 [2.2]	50 ± 5	80 ± 18
	1900	10	141 ± 58 [1.8]	98 ± 42 [1.7]	121 ± 56 [2.1]	45 ± 7	78 ± 23
Foot (plantar flexor)	1000	7	70 ± 28 [1.6]	35 ± 13 [1.3]	48 ± 27 [1.7]	59 ± 8	78 ± 22
	1500	7	80 ± 28 [1.5]	45 ± 11 [1.2]	51 ± 24 [1.3]	59 ± 12	78 ± 16
	1900	9	105 ± 46 [1.3]	57 ± 20 [1.0]	79 ± 50 [1.3]	62 ± 5	75 ± 15
Forearm (ulnar flexor)	1000	9	43 ± 19	28 ± 18	28 ± 15	39 ± 14	68 ± 22
	1500	7	53 ± 23	37 ± 22	39 ± 24	41 ± 13	69 ± 20
	1900	8	79 ± 27	58 ± 38	59 ± 40	30 ± 10	62 ± 10

*Population averages are presented with standard deviations for the peak, mean flow rates, and total hyperemic flow volume, along with the time to peak and hyperemic peak width at the three tested postlabeling delays (PLDs). Except for time to peak and hyperemic duration, the number in brackets is the ratio of mean of each flow measure to the mean flow measure in forearm flexors.

Table 2

Summary of Statistical Analysis*

	P value		
	ROI	**PLD**	**ROI × PLD**
Peak flow	<0.0001	<0.0001	0.39
Mean flow	<0.0001	<0.0001	0.32
Total flow	<0.0001	<0.0001	0.39
Time to peak	<0.0001	0.33	0.31
Peak width	0.045	0.80	0.85

*Results of the two-way ANOVA with interaction effect analysis, which tested the dependence of the measured variables: peak flow, mean flow, total flow, time to peak, and peak width upon the region of interest (ROI) or muscle group, the postlabeling delay (PLD) and the interaction between these variables, ROI × PLD. *P* values are listed to indicate the significance level for the effect of the ROI, PLD, or their interaction upon the measured variables.